

## Formulation and *in vitro* Evaluation of Acemetacin Nanosuspension

Hussein Al-Gharani<sup>1</sup>   and Khalid Al-Kinani<sup>\*,2</sup>  

<sup>1</sup>Ministry of Health and Environment, Karbala Health Directorate, Karbala, Iraq.

<sup>2</sup>Department of Pharmaceutics, College of Pharmacy, University of Baghdad, Baghdad, Iraq.

\*Corresponding Author.

Received 26/3/2024, Accepted 10/7/2024, Published 15/2/2025



This work is licensed under a Creative Commons Attribution 4.0 International License.

### Abstract

Acemetacin (ACM) is classified as a non-steroidal anti-inflammatory drug (NSAID). It is an indomethacin glycolic ester that is transformed into indomethacin *in vivo*. The analgesic, antipyretic, and anti-inflammatory properties of the ACM are attributed to its prostaglandin inhibitory action. Acemetacin belongs to biopharmaceutical classification system (BCS) class II drugs, which are characterized by having high permeability but poor aqueous solubility. The purpose of this study was to develop acemetacin nanosuspension for the enhanced rate of dissolution. The solvent-anti-solvent approach was used to formulate the nanosuspension. Two stabilizers were used to prepare ACM nanosuspension (sodium deoxycholate (SDC) and Soluplus®). Acemetacin was dissolved in ethanol, added drop by drop to the anti-solvent containing a particular amount of stabilizer, and stirred at a certain rate using a hot plate magnetic stirrer. Design Expert® software was used to create the experiments utilizing a computer-based approach. The Box-Behnken design was used for this purpose to investigate the effect of different formulation variables on the particle size and polydispersity index (PDI) of ACM nanosuspension. Using Soluplus® as a stabilizer, the chosen formula F22 has a desirability value of 0.701, and its particle size and PDI values were 59.69 nm and 0.1847 respectively. The saturated solubility of ACM in the generated nanosuspension was approximately ten times greater than that of the pure drug (25.01 µg/ml vs. 2.43 µg/ml), and a 58.9% dissolution was achieved in 30 minutes compared to the pure ACM, which only gave 21.9% in this time frame. In conclusion, Acemetacin nanosuspension can be successfully developed using the solvent-anti-solvent approach. Turning ACM into nanosuspension is an effective method to increase the rate of dissolution of the drug, and make a uniform dispersion readying it for incorporation into a dosage form requiring such properties with high content uniformity.

**Keywords:** Acemetacin nanosuspension, Box-Behnken design, Sodium deoxycholate, Soluplus®, Solvent-anti-solvent.

### Introduction

Drugs with low aqueous solubility represent about one-third of the drugs listed in the United States Pharmacopeia (USP). Poor aqueous solubility is a recurrent challenge in formulating and optimizing pharmaceutical dosage forms <sup>(1)</sup>.

Drugs with low water solubility are classified as class II or class IV in the Biopharmaceutics Classification System (BCS). The BCS class II drugs have high permeability and limited solubility. There are numerous techniques including particle size reduction, salt formation, inclusion complexes, pH modification, hydrotrophy, solid dispersion, cocrystal, amorphous compound production, and nanosization that can solve the problem of the BCS class II drugs' poor solubility <sup>(2)</sup>.

Nanosization is the process of reducing the drug particle size to the nanoscale to form nanoparticles, which are drug particles with sizes ranging from 10 to 1000 nanometers (nm). Because of their small sizes, the nanoparticles will have a

higher surface area, which will enhance their solubility <sup>(3)</sup>.

Nanoparticles display several advantages over conventional formulations where they possess: better stability of chemically labile drugs, greater drug loading, enhanced targeting ability, and higher dissolution rate and solubility of poorly soluble drugs <sup>(4)</sup>.

Nanosuspension is the colloidal dispersion of nano-sized drug particles generated by a suitable technique and stabilized with a suitable stabilizer. Converting a drug into a nanosuspension for oral administration may increase its absorption. In addition to improving oral absorption, nanosuspensions have other benefits, such as improved dose proportionality, reduced fed/fasted state variability, lower inter-subject variability, and faster onset of action for medications that are completely but slowly absorbed <sup>(1)</sup>. Nanosuspension preparation involves various methods like solvent-

antisolvent, high-pressure homogenization, media milling, etc. Stability is a major issue due to its small and high surface area, leading to aggregation called Ostwald ripening. Stabilizers prevent agglomeration, enhancing stability<sup>(5,6)</sup>.

Acemetacin (ACM) is a BCS class II NSAID, a glycolic ester of indomethacin converted in vivo. It exhibits analgesic, antipyretic, and anti-inflammatory effects through prostaglandin inhibition. Its efficacy stems from both the prodrug and major metabolite, treating various conditions like osteoarthritis, rheumatoid arthritis, and postoperative pain<sup>(7)</sup>. Acemetacin causes significantly less gastrointestinal damage than indomethacin<sup>(8)</sup>.

Acemetacin is a yellowish light-sensitive crystalline powder. It is practically insoluble in water, slightly soluble in ethanol, and insoluble in acetone. The molecular weight of ACM is 415.8 g/mol<sup>(7)</sup>. ACM is a strong acid with a pKa value ranging from 2.6 to 3.57. The melting point ranges from 150 to 151.3 °C, and also displays polymorphism<sup>(9,10)</sup>.

Acemetacin has previously been prepared using nanotechnology-related approaches. Shehata, Abdallah, et al. (2015) produced acemetacin as proniosomal tablets. They showed better acemetacin pharmacokinetic properties, such as AUC, Tmax, half-life, and relative bioavailability. Shewaiter, Selim, et al. (2022) conducted a radio-kinetic study of acemetacin as an intravenous niosomal formula to improve acemetacin tumor targeting<sup>(11,12)</sup>.

The primary objective of this study is to fabricate a nanosuspension of acemetacin using the solvent-anti-solvent method, aimed at enhancing its dissolution rate and making a uniform dispersion readying it for incorporation into a dosage form requiring such properties with high content uniformity. Additionally, the investigation will probe into the impact of various formulation parameters on the process to attain the most favorable physicochemical attributes.

## Materials and Methods

### Materials

Pure acemetacin was purchased from Bidepharm, Shanghai, China. Soluplus® was

purchased from BASF SE, Ludwigshafen, Germany. Sodium deoxycholate (SDC) was purchased from Baoji Guokang Bio-technology Co., Ltd., Shanxi, China. Potassium Dihydrogen Phosphate (KH<sub>2</sub>PO<sub>4</sub>) and Disodium Hydrogen Phosphate (Na<sub>2</sub>HPO<sub>4</sub>) were purchased from Panreac, Barcelona, Spain. Ethanol was purchased from BDH Chemical Ltd., England. The dialysis membrane M.W. 8000–14000 was purchased from Special Products Laboratory, USA, and the Amicon ultra centrifugal filter was purchased from Merck KGaA, Darmstadt, Germany.

### Methods

#### Preparation of ACM nanosuspension

The solvent-antisolvent method was used to prepare ACM nanosuspension formulas. The organic phase was prepared by dissolving 30mg of ACM in 3 milliliters of ethanol 99% at 37 °C. The aqueous phase was prepared by dissolving a certain amount of a stabilizer in various quantities of distilled water, then stirred on a hot plate magnetic stirrer at different stirring rates. The organic phase is added drop by drop to the whirling aqueous phase using a 27G needle syringe at a rate of 0.5 milliliter per minute. The suspension was left on the magnetic stirrer for one hour which was long enough for the entire organic solvent to evaporate<sup>(13)</sup>.

#### Computer-based experimental model

For the formulation of study formulas, we utilized Design-Expert®, a software tailored for scientific experimentation across various models. Specifically, we employed the Box-Behnken model for its robustness and efficiency<sup>(14)</sup>. This model allowed us to explore the impact of independent variables, namely (A) stabilizer amount, (B) anti-solvent volume, (C) stirring speed, and (D) stabilizer type, on the responses, which were (response 1) particle size and (response 2) polydispersity index (PDI), as detailed in Table 1. A comprehensive set of thirty-two formulas was generated by the Box-Behnken model, as outlined in Table 2.

**Table 1. Factors and responses used in the Box-Behnken model**

Independent variables	Levels	Responses
A: stabilizer amount	30 mg, 45 mg, and 60 mg.	Particle size PDI
B: anti-solvent volume	10 ml, 15 ml, and 20 ml.	
C: stirring speed	500 rpm, 1000 rpm, and 1500 rpm.	
D: stabilizer type	Soluplus® or sodium deoxycholate (SDC)	

SDC (sodium deoxycholate)

Table 2. Formulas suggested by the Box-Behnken model

Formula	ACM (mg)	Stabilizer amount(mg)	Anti-solvent Volume (milliliters)	Stirring speed(rpm)	Stabilizer type
F1	30	60	15	500	SDC
F2	30	30	10	1000	SDC
F3	30	60	10	1000	SDC
F4	30	45	10	500	Soluplus®
F5	30	30	15	1500	SDC
F6	30	45	10	500	SDC
F7	30	30	10	1000	Soluplus®
F8	30	30	15	1500	Soluplus®
F9	30	45	15	1000	SDC
F10	30	45	10	1500	SDC
F11	30	45	10	1500	Soluplus®
F12	30	60	15	1500	SDC
F13	30	45	20	500	Soluplus®
F14	30	60	20	1000	SDC
F15	30	45	20	1500	SDC
F16	30	60	15	1500	Soluplus®
F17	30	45	20	500	SDC
F18	30	45	20	1500	Soluplus®
F19	30	45	15	1000	Soluplus®
F20	30	60	15	500	Soluplus®
F21	30	60	10	1000	Soluplus®
F22	30	60	20	1000	Soluplus®
F23	30	30	20	1000	Soluplus®
F24	30	30	20	1000	SDC
F25	30	30	15	500	Soluplus®
F26	30	30	15	500	SDC
F27	30	45	15	1000	Soluplus®
F28	30	45	15	1000	Soluplus®
F29	30	45	15	1000	Soluplus®
F30	30	45	15	1000	SDC
F31	30	45	15	1000	SDC
F32	30	45	15	1000	SDC

### Characterization of ACM nanosuspension

#### Measurement of particle size and polydispersity index (PDI)

The particle size and PDI of the ACM nanosuspension formulas were measured using the dynamic light scattering method<sup>(15)</sup>. The device used was a particle size analyzer nanolaser (Malvern Zeta sizer) manufactured by Spectris Company in the United Kingdom. one milliliter of each sample (F1-F32) was poured into a polystyrene zeta cell. The light scattering was recorded at 25 °C (90 °angle)

#### Determination of ACM entrapment efficiency in nanosuspension formulas

The indirect method (that depends on measuring the concentration of free (unbound) drug that has dissolved in the dispersion medium) was used. Four milliliters of the nanosuspension formula were centrifuged at 4000 rpm for thirty minutes using an Amicon® ultra centrifugal filter. One milliliter was withdrawn from the filtrate in the lower compartment of the centrifugal filter and

measured with a UV spectrometer (Shimadzu, Japan) at  $\lambda$  max equal to 318 nm using distilled water as a blank and the concentration was determined from a calibration curve previously constructed for this purpose ( $y= 0.0173x - 0.0297$ , and  $R^2 = 0.9999$ ). The percentage of entrapment efficiency (%EE) was calculated according to equation 1<sup>(16)</sup>:

$$\%EE = \frac{(total\ drug\ in\ formula - amount\ of\ free\ drug) \times 100}{total\ drug\ in\ formula} \quad (1)$$

#### Determination of drug content

The drug content test was performed on the nanosuspension formulae to calculate the actual amount of acemetacin in each formula as compared to the theoretical value. A certain volume of nanosuspension (one milliliter) was transferred into a volumetric flask filled with 10 ml ethanol. The mixture was sonicated for one hour and filtered through a 0.45-micron syringe filter. The filtrate was then analyzed using a UV spectrophotometer to

determine the amount of ACM using the ACM calibration curve constructed for this purpose ( $y = 0.0155x - 0.0087$ , and  $R^2 = 0.999$ )<sup>(17)</sup>.

#### ***In-vitro dissolution of ACM nanosuspension***

The dissolution test of ACM nanosuspension was conducted in a USP type II dissolution apparatus. The nanosuspension was placed in a pre-soaked dialysis bag immersed in phosphate buffer pH 6.8. The dialysis bag was anchored to the paddle using a thread. The paddle was rotated at 100 rpm in 1000 milliliters of phosphate buffer pH 6.8 at a temperature of 37 °C. Samples were withdrawn at intervals (5, 10, 15, 20, 35, 40, 45, 60, 75 and 90 minutes) and replaced with fresh media. The concentration of ACM released was measured using a UV spectrophotometer ( $y = 0.0175x - 0.0352$ , and  $R^2 = 0.9992$ ). Dissolution profiles were generated by plotting cumulative drug release against time intervals<sup>(18)</sup>.

The percentage of acemetacin released within 30 minutes was calculated for each nanosuspension formula and compared to that of a pure acemetacin suspension<sup>(19)</sup>.

#### ***Selected formula***

The selected ACM nanosuspension formula was determined by taking into account multiple factors such as particle size, PDI, entrapment efficiency, zeta potential, and in-vitro release of the formula in PBS pH 6.8.

#### ***Freeze-drying of the selected formula of ACM nanosuspension***

Initially, the selected nanosuspension formula was freeze-dried using Christ Alpha 1-2 LDplus freeze dryer, Germany. Liquid nitrogen was first used to freeze the formula to a temperature of around -70 °C. Then, the frozen formula was transported to a vacuum freeze dryer to be lyophilized. Ice was sublimated from the frozen formula during the lyophilization process in two stages: primary drying (0.021 millibars at -50°C) and secondary drying (6.1 millibars at 0 °C). The lyophilization process continued until a dry, light, and easily crushed powder was obtained. The dried ACM nanosuspension was used for subsequent examinations that required the formula to be in dry form, such as differential scanning calorimetry and powder x-ray diffraction<sup>(20)</sup>.

#### ***Characterization of ACM selected formula***

##### ***Measurement of zeta potential of the best formula***

The Malvern Zeta Sizer, UK, was used to measure the zeta potential of the selected ACM nanosuspension formula. One milliliter of the sample was injected into a capillary zeta cell, and the measured zeta potential value was recorded<sup>(21)</sup>.

#### ***Determination of saturated solubility of the best formula***

The saturated solubility of the freeze-dried selected formula and the pure drug were determined using the shake flask method<sup>(22)</sup>. An excess amount was added to a 10-milliliter tube containing distilled water. The mixture was shaken for 48 hours in a water bath shaker at 25 °C. After that, the mixture was filtered by a 0.45µm filter syringe and dissolved ACM concentration was measured using a UV spectrophotometer.

#### ***Crystallinity analysis using X-ray diffraction technique***

The powder x-ray diffraction method (PXRD) was used to determine the crystalline structures of the lyophilized ACM nanosuspension, physical mixture (ACM and stabilizer), and the pure drug<sup>(23)</sup>. The x-ray diffraction patterns were collected using Shimadzu XRD-6000, Japan operating at a voltage of 40 Kv and a current of 30 mA while running in continuous scan mode with a range of 2 to 60 degrees and a step size of 0.05 degrees at a speed of 5 degrees per minute.

#### ***Determination of surface morphology by scanning electron microscopy***

The surface morphology of both pure ACM and the lyophilized selected formula was examined by Nano-Lab, USA scanning electron microscope. When examining the surface morphology of the pure drug and the lyophilized formula, the powder was directly placed on double-sided carbon tape and coated with gold<sup>(24)</sup>.

#### ***Determination of drug excipients compatibility study***

##### ***Fourier Transform Infrared Spectroscopy (FTIR)***

The Fourier transform infrared spectroscopy (FTIR) spectrums of the pure drug, Soluplus®, selected formula physical mixture, and ACM lyophilized nanosuspension (selected formula) were obtained using Shimadzu FTIR spectrophotometer, Japan. Each material was mixed with potassium bromide powder (KBr) and compressed into a thin film disc, then the sample was analyzed using infrared radiation at a wavenumber of 4000-400 cm<sup>-1</sup><sup>(25)</sup>.

##### ***Differential Scanning Calorimetry (DSC)***

Differential scanning calorimetry (DSC) determines the thermodynamic changes of the drug as a function of time and temperature. The thermograms of ACM and ACM lyophilized nanosuspension of the selected ACM nanosuspension formula were obtained using Shimadzu DSC-60, Japan apparatus. About 5 mg of each sample was placed into an aluminum pan, sealed by crimping and heated at a constant heating rate of 10 C°/min. Nitrogen gas was pumped at a flow rate of 20 ml/min to maintain an inert environment<sup>(26)</sup>.

## Results

### *Particle size and polydispersity index of the prepared ACM nanosuspensions*

The combination of factors used in the preparation of nanosuspension (stabilizer amount, anti-solvent volume, stirring speed, and polymer type) resulted in the formation of a suspension of particle size ranging from 59.69-6459 nm as shown in Table 3. Sixteen of the thirty-two formulas fell within the agreed nanosuspension particle size range for pharmaceutical uses (below 200 nm) <sup>(27)</sup>.

On the other hand, the PDI which is the measure of sample homogeneity ranged from 0.0145 to 0.9491 as shown in Table 3. A polydispersity index values of 0 to 0.05 indicate a highly monodispersed system, PDI values of 0.05 to 0.7 indicate a mid-range polydispersed system, and PDI values of 0.7 to 1 indicate a highly polydispersed system. For nanosuspension, values of 0.2 and below are often acceptable <sup>(28)</sup>. Therefore, twenty-two out of thirty-two of the prepared formulas were homogenous size systems.

**Table 3. Particle size and PDI of the prepared ACM nanosuspensions**

Formula	Particle size (nm)	PDI	Formula	Particle size (nm)	PDI
F1	450.7	0.122	F17	1065	0.5686
F2	4907	0.397	F18	65	0.2353
F3	423	0.1072	F19	64.45	0.1545
F4	67.98	0.223	F20	62.59	0.1282
F5	3385	0.2239	F21	60.67	0.1759
F6	2491	0.8206	F22	59.69	0.1847
F7	69.23	0.1533	F23	71.06	0.087
F8	65.78	0.089	F24	3497	0.9491
F9	483.5	0.0434	F25	75.51	0.08
F10	409.1	0.047	F26	6459	0.0145
F11	60.72	0.13	F27	64.3	0.0823
F12	654	0.0561	F28	70.44	0.1164
F13	59.83	0.0717	F29	62.2	0.0998
F14	436	0.0763	F30	431.4	0.471
F15	516.4	0.0679	F31	403.2	0.4436
F16	64.77	0.1855	F32	371.4	0.4727

### *Analyzing the particle size and PDI values*

The experimental design is currently considered a common method to analyze the effects of different factors on the properties of pharmaceutical formulations <sup>(29)</sup>.

In this study, stabilizers and other independent factors were chosen depending on preliminary study results. An analysis model called the design model has been recommended by the Box-Behnken design and it was a significant model ( $P < 0.001$ ) for the analysis of the particle size. The adequate precision value was greater than four (62.02), which means the selected analysis model was effective. Also, the predicted  $R^2$  value (0.9604) was in reasonable agreement with the adjusted  $R^2$  value (0.9934) as the difference was less than 0.2. However, in the analysis of the PDI values, the design model was not significant <sup>(30)</sup>.

### *Factors influencing particle size and PDI values in the produced formulas.*

#### *The effect of Stabilizer type on particle size and PDI*

By using the ANOVA test, the stabilizer type (Soluplus® or SDC) has a significant effect on

particle size with a p-value equal to 0.0018 ( $P < 0.05$ ). The formulas prepared by using Soluplus® polymer have a much smaller particle size than SDC formulas.

The stabilizer type (parameter D) also has a significant effect on the polydispersity index (p-value  $< 0.05$ ), as Soluplus® formulas showed lower PDI values than SDC formulas.

#### *The effect of stabilizers amount, stirring speed, and anti-solvent volume on the particle size of ACM nanosuspension*

The amount of stabilizer (parameter A) has a significant effect (p-value  $< 0.0001$ ) on the particle size of ACM nanosuspension. As the stabilizer amount increases, the particle size decreases.

The anti-solvent volume (variable B) also has a significant effect on the particle size of ACM nanosuspension formulas ( $P < 0.05$ ).

Even stirring speed (variable C) has a significant effect on the particle size of ACM nanosuspension formulas ( $P < 0.0001$ ). The effect of stabilizer amount, anti-solvent volume, and stirring speed on the particle size of ACM nanosuspension formulas is depicted in Figure 1.

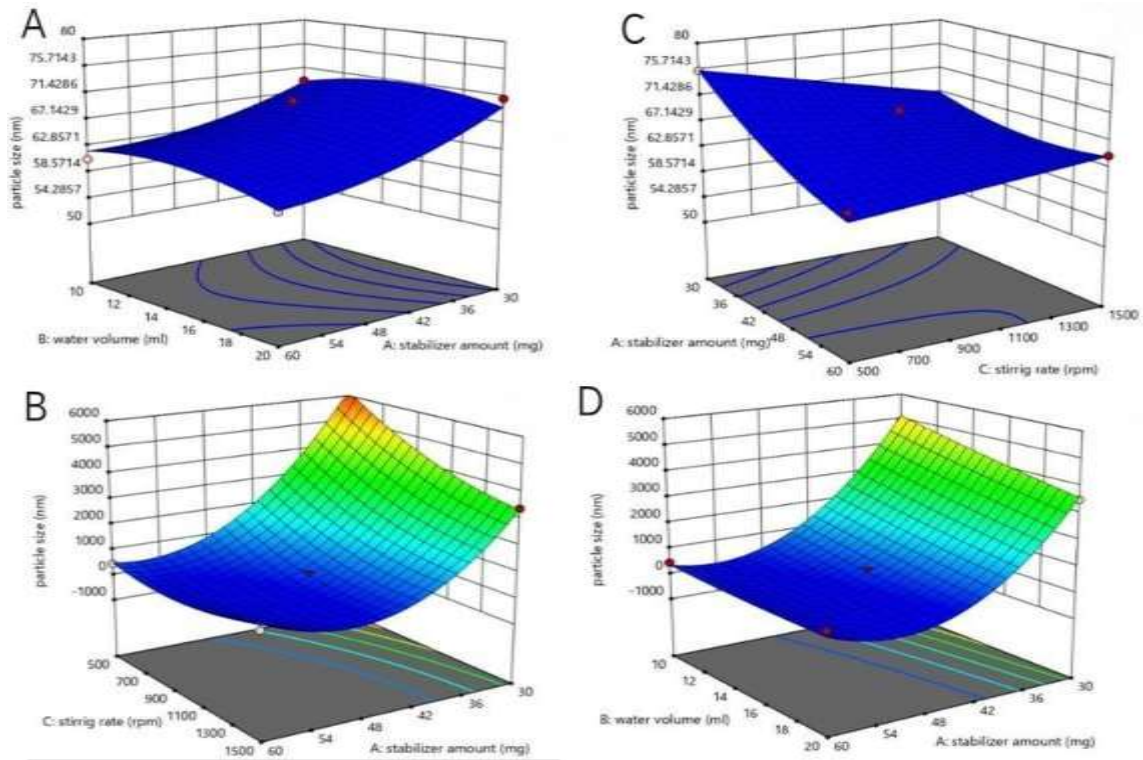


**Figure 1.** 3D surfaces describe the effect of stabilizer amount, anti-solvent volume, and stirring speed on the particle size of ACM nanosuspension formulas: Soluplus® formulas (A and B) and SDC formulas (C and D)

*The effect stabilizer amount, anti-solvent volume, and stirring speed on the polydispersity index (PDI) of the prepared ACM nanosuspension formula*

The stabilizer amount (variable A), anti-solvent volume (variable B), and stirring speed (variable C) have no significant effect on PDI values as the P value is higher than 0.05.

*Optimization of the ACM nanosuspension-prepared formulas*

The optimization criteria include low particle size (below 200 nm) and a PDI in the range of 0-0.2. The best five ACM nanosuspension formulas were F11, F16, F20, F21, and F22. They were selected depending on their desirability values as shown in Table 4.

**Table 4.** The desirability values of the best five formulas.

Formula	Description of each formula	Desirability*	Measured particle size\predicted particle size
F16	ACM 30 mg, Soluplus® 60 mg, an anti-solvent volume of 15 ml, and a stirring rate of 1500 rpm.	0.676	64.77\64.70
F22	ACM 30 mg, Soluplus® 60 mg, an anti-solvent volume of 20 ml, and a stirring rate of 1000 rpm.	0.701	59.69\59.85
F21	ACM 30 mg, Soluplus® 60 mg, an anti-solvent volume of 10 ml, and a stirring rate of 1000 rpm.	0.690	60.67\62.01
F20	ACM 30 mg, Soluplus® 60 mg, an anti-solvent volume of 15 ml, and a stirring rate of 500 rpm.	0.694	62.59\61.16
F11	ACM 30 mg, Soluplus® 45 mg, an anti-solvent volume of 10 ml, and a stirring rate of 1500 rpm.	0.703	60.72\59.45

\*Desirability values are given by the software according to the optimization criteria.

**Drug content and entrapment efficiency**

The ACM content values of the best five nanosuspension formulas ranged from 96.1% to 99.4%, as shown in Table 5. On the other hand, %

entrapment efficiency calculated via the indirect method for the best five nanosuspension formulas is also shown in Table 5 and ranged from 96.3% to 98.6%, with the highest value shown for F22.

**Table 5. ACM content and % entrapment efficiency of the optimal formulas**

Formula	ACM content (%)	% entrapment efficiency
F11	98.5%	96.3%
F16	98.4%	96.9%
F20	99.4%	97.1%
F21	98.7%	97%
F22	96.1%	98.6%

**In-vitro drug release study of ACM nanosuspension**

In-vitro dissolution profiles of the pure ACM suspension and ACM nanosuspension formulas are

shown in Figure 2, while the percentages of acemetacin released within 30 minutes for the pure drug suspension and the best five ACM nanosuspension formulas are illustrated in Table 6.

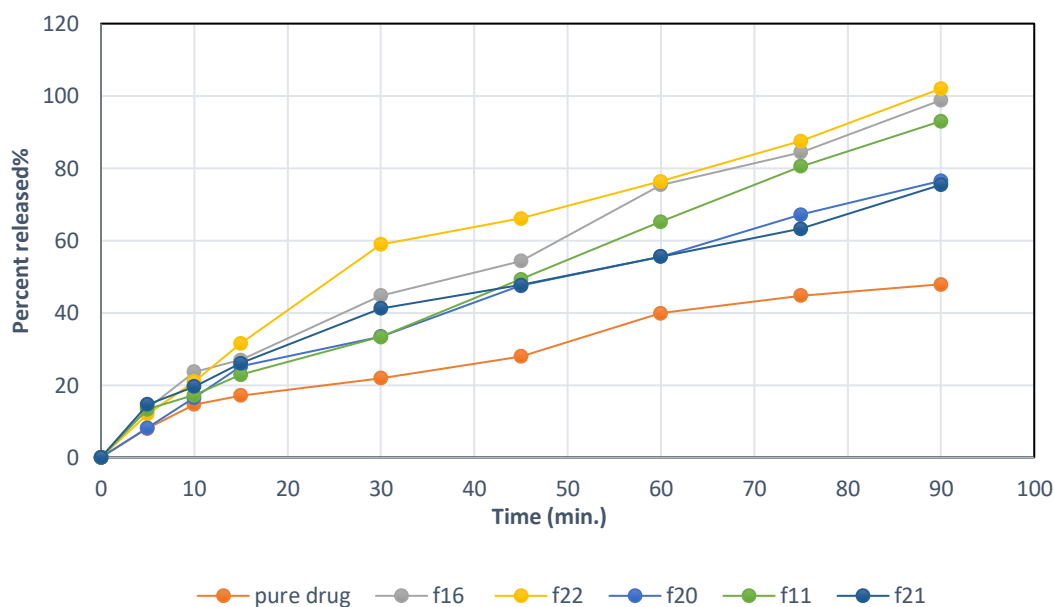


**Figure 2. In-vitro release profiles of the best ACM nanosuspension formulas as compared to the pure drug suspension in phosphate buffer pH 6.8 media**

**Table 6. The percentages of acemetacin released within 30 minutes for the pure drug suspension and the best five ACM nanosuspension formulas**

Formula	The percentages of acemetacin released within 30 minutes
F16	44.8%
F22	58.9%
F20	33.3%
F11	33.4%
F21	41.22%
Pure ACM suspension	21.9%

**Determination of the ACM nanosuspension selected formula**

The formula F22 was determined as the selected formula based on its particle size (59.69

nm), polydispersity index (0.1847), in-vitro release profile (58.9% in 30 minutes), drug content (96.1%), and % entrapment efficiency (98.6%) to be subjected for further characterization.

### Characteristics of the selected formula (F22) Zeta potential and saturated solubility

The zeta potential was equal to -18 mv, and the saturated solubility of F22 in water was 25.01  $\mu\text{g/ml}$ , 10.29 times higher than that of the pure ACM (2.43  $\mu\text{g/ml}$ )<sup>(31)</sup>.

### Fourier transform infrared spectroscopy

The Fourier transform infrared spectroscopy (FTIR) of the pure ACM, Soluplus®, Physical mixture (Soluplus® 60mg and ACM 30 mg), and F22 formula are shown in Figure 3. Also, their most characteristic peaks are illustrated in Table 7. The most characteristic peaks were compared with the reference ACM FTIR spectrum

<sup>(32)</sup>. The spectra of the physical mixture and F22 showed the characteristic peaks of ACM which are the carbonyl stretching peaks at 1749.44  $\text{cm}^{-1}$  and 1724.36  $\text{cm}^{-1}$  (which were visible in the physical mixture spectrum and obscured by the Soluplus® carbonyl stretching peak at 1735.93  $\text{cm}^{-1}$  in the F22 formula spectrum), the carbonyl stretching peaks of amide and aromatic C=C at 1662.64  $\text{cm}^{-1}$  and 1610.56  $\text{cm}^{-1}$ , the hydroxyl stretching peak at 3473.8  $\text{cm}^{-1}$ , and the C-O-C ether stretching peak at 1230.58  $\text{cm}^{-1}$ . The small shift in the peak positions in the formula F22's FTIR spectrum could be due to hydrogen bond formation<sup>(33)</sup>.

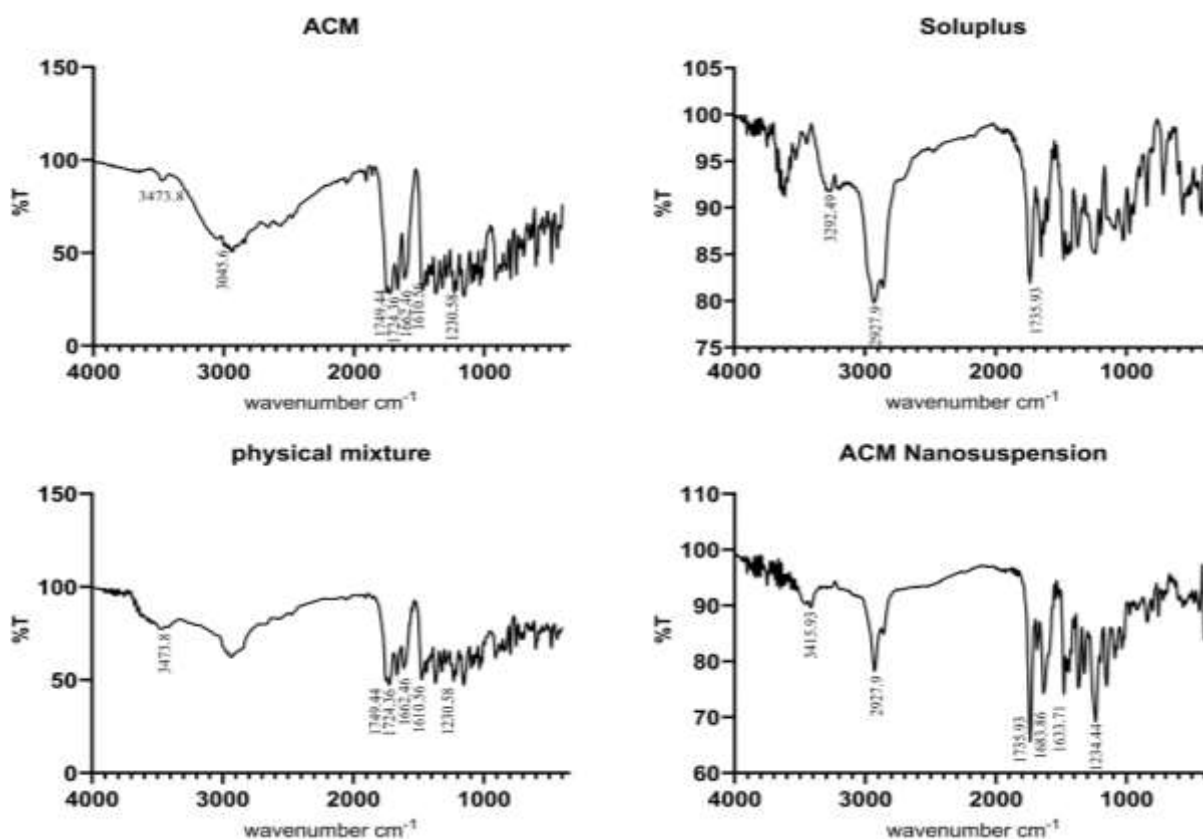


Figure 3. FTIR spectra of pure ACM, Soluplus®, physical mixture, and ACM lyophilized nanosuspension (F22).

Table 7. FTIR's most characteristic peaks are pure ACM, physical mixture, and F22 lyophilized nanosuspension

Functional group	Peak value ( $\text{cm}^{-1}$ )		
	pure ACM	physical mixture	F22 lyophilized nanosuspension
C=O stretching	1749.44, and 1724.36	1749.44, and 1724.36	-
C=O amide and Aromatic C=C stretching	1662.64, and 1610.56	1662.64, and 1612.49	1683.86, and 1633.71
O-H stretching	3473.80	3473.80	3415.93
C-O-C ether stretching	1230.58	1230.58	1234.44

**Powder X-ray diffraction**

X-ray diffraction (XRD) patterns of the pure ACM, physical mixture, and the lyophilized ACM nanosuspension are shown in Figure 4. Figure 4A shows that the pure ACM diffraction pattern has distinct Bragg peaks with intensities of 560, 652,

786, and 580 at 2 theta angle ( $2\theta$ ) of 11.95, 16.7, 19.05, and 22.25, respectively. These peaks can also be seen in the physical mixture's XRD pattern (Figure 4B), but they are much less noticeable in the lyophilized ACM nanosuspension XRD pattern (Figure 4C).

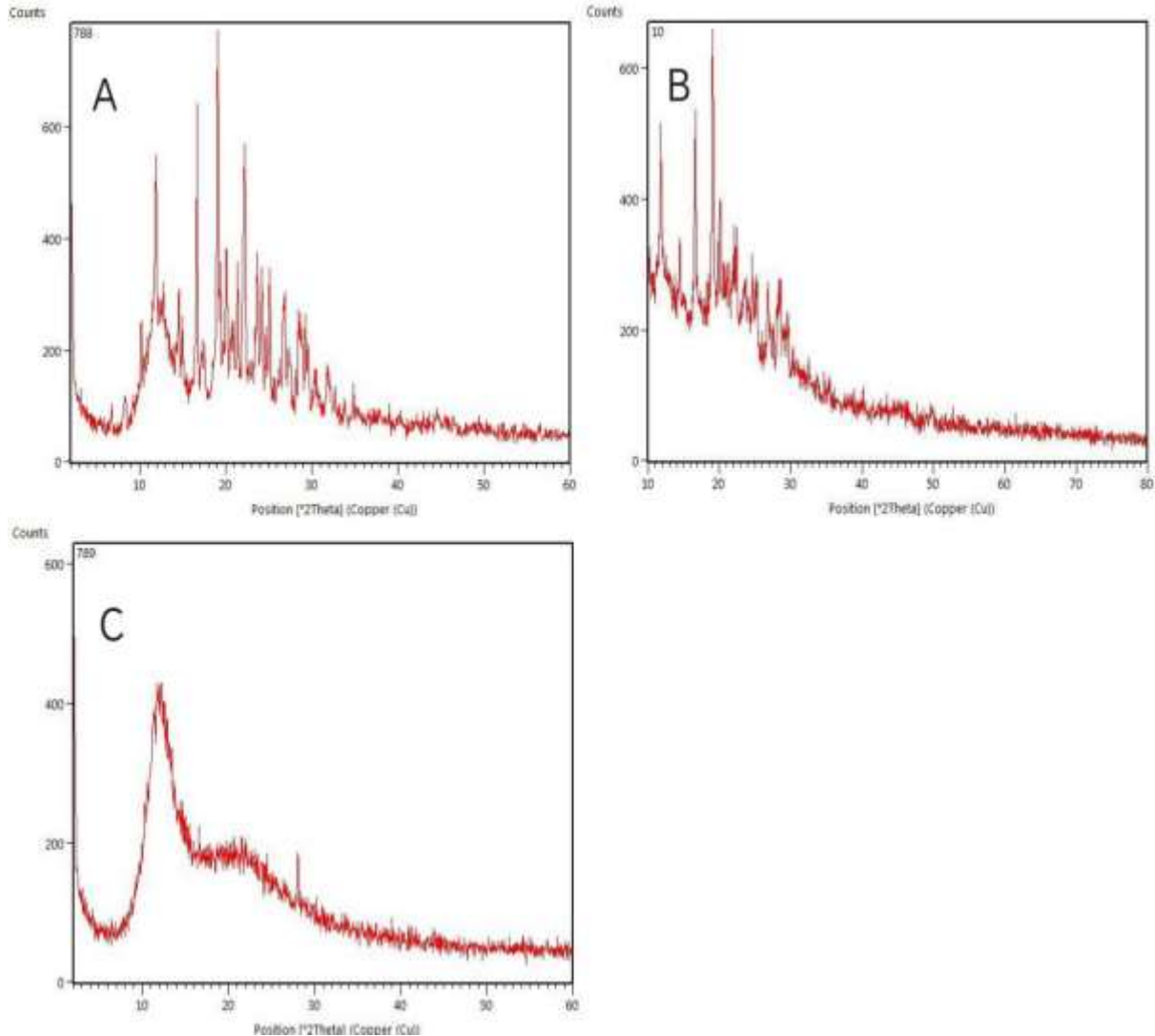


**Figure 4. Powder X-ray diffraction of (A) pure ACM, (B) physical mixture, and (C) ACM lyophilized nanosuspension.**

**Scanning electron microscopy**

Scanning electron microscopy of pure ACM and F22 lyophilized nanosuspension is shown in Figure 5. Figures 5A and 5B show the crystalline form of the pure ACM at a magnification power of 1.00 kx and 20.0 ks, respectively, which resemble

tetragonal prisms. Figures 5C and 5D show the surface morphology of the ACM-lyophilized nanosuspension at a magnification power of 1.00 kx and 20.0 ks, respectively, which appeared as smaller, flakey particles.

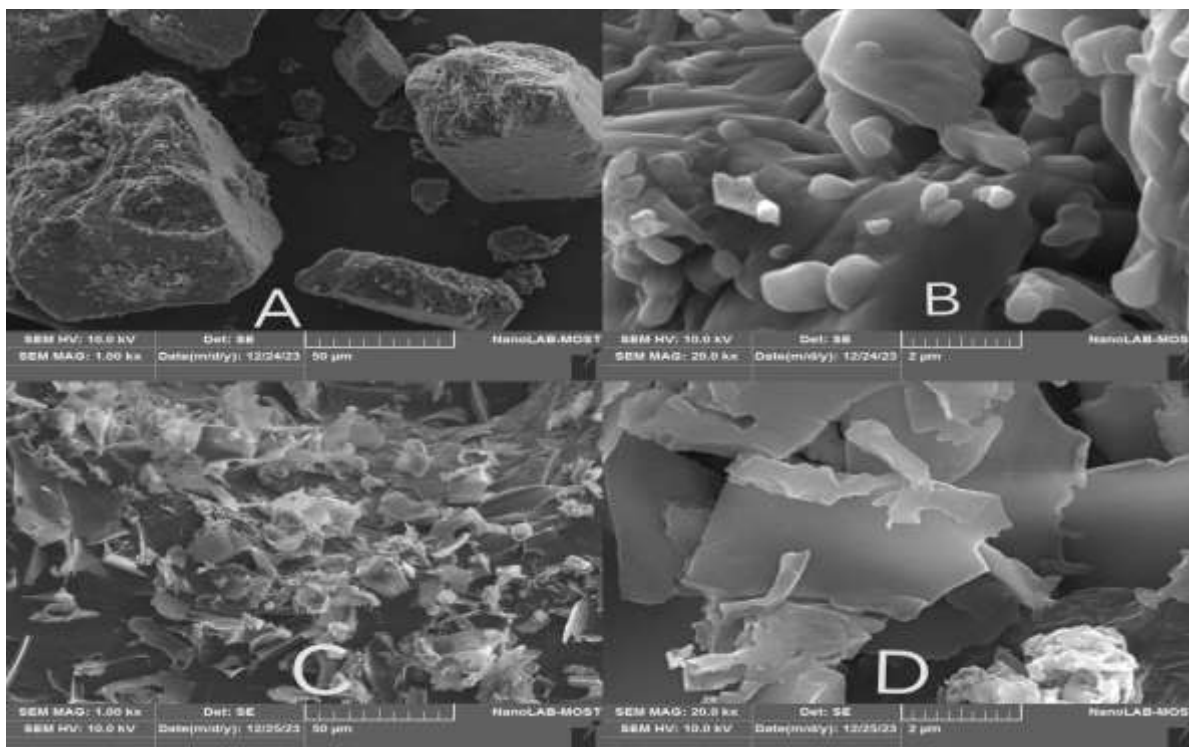


**Figure 5. SEM of (A) pure ACM (MAG:1.00 kx), (B) pure ACM (MAG 20.0 kx), (C) ACM lyophilized nanosuspension (MAG 1.00 kx), and (D) ACM lyophilized nanosuspension (MAG 20.0 kx)**

**Differential scanning calorimetry**

Figure 6 displays the differential scanning calorimetry (DSC) thermograms of the physical mixture, pure ACM, and ACM lyophilized nanosuspension (F22). A prominent endothermic peak is shown at 149.54 °C on the DSC thermogram of the pure ACM (Figure 6A), which is nearly at the same position within the ACM

melting point range <sup>(34)</sup>. A peak at 154.26 °C, which is also close to the melting point range of ACM, is seen in the DSC of the physical mixture of acemetacin and Soluplus® in a ratio of 1:2 (Figure 6B). In the DSC thermogram of ACM lyophilized nanosuspension (Figure 6C), the ACM endothermic peak has completely disappeared.

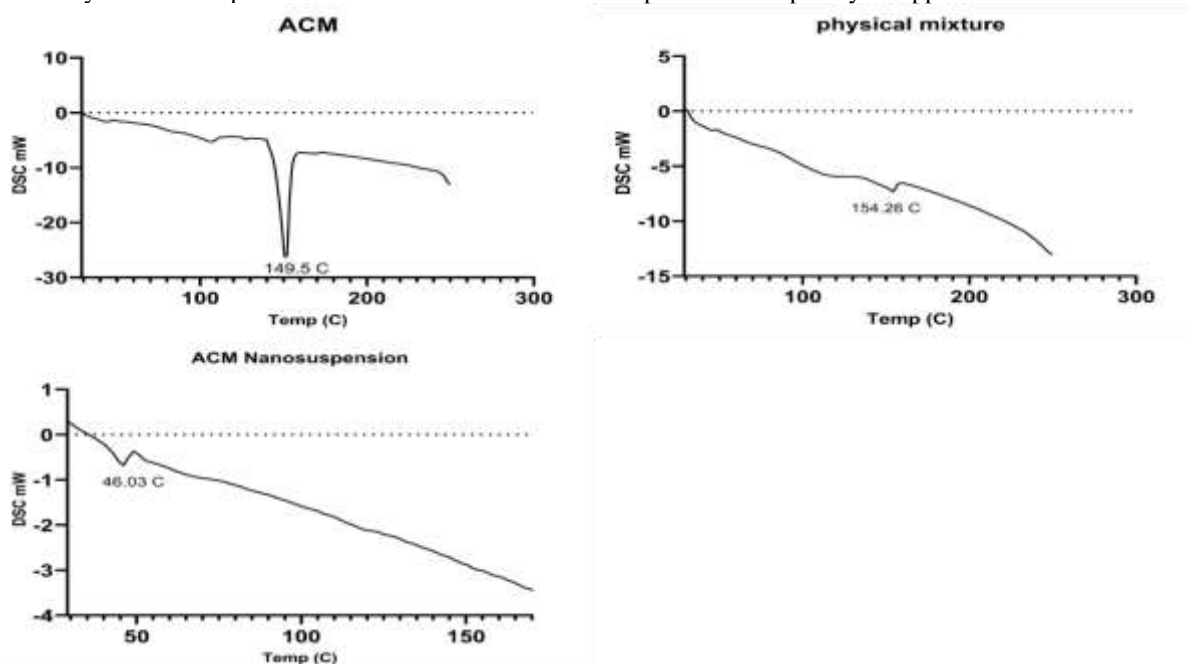


**Figure 6. DSC thermograms of pure ACM, physical mixture, and ACM lyophilized nanosuspension.**

## Discussion

### *The effect of the Independent variables on the particle size and PDI values*

The Soluplus® formulas have smaller particle size and PDI values than SDC formulas as Soluplus®'s exceptional amphiphilic property contributes to its high wettability and surface activity. Thus, by permitting attractive water-surfactant interaction, Soluplus® lowers the interfacial tension of the particle surface and ensures the presence of small particles in nanosuspension<sup>(35)</sup>.

As the stabilizer amount increases the particle size decreases. Theoretically, sufficient steric repulsion between the crystals requires total adsorption and polymer covering on the surface of the freshly created crystals. Therefore, sufficient stabilizers in the precipitation system can meet the need to restrict crystal formation and, as a result, prevent crystal agglomeration<sup>(36)</sup>.

The mean particle size increased as the antisolvent volume was reduced. This phenomenon could be explained by the fact that during the precipitation process, growth started as soon as the crystal nucleus formed. So, the formulas with high anti-solvent volumes will have a lower drug concentration and a smaller particle size formation<sup>(37)</sup>.

As the stirring speed increases the particle size decreases. The high-speed agitation with a magnetic stirrer ensures rapid nucleation and also breaks down drug crystals, which prevents the crystals from getting larger<sup>(38)</sup>.

### *In-vitro characterization results of ACM nanosuspension best formula (F22)*

The measurement of the zeta potential produced a result of -18 mV. This can be explained by the steric stabilizer Soluplus®, which used steric hindrance to efficiently stabilize the ACM nanosuspension. As a result, the ACM nanosuspension ' charge was hidden by the stabilizer, which enveloped them<sup>(39)</sup>. Even at zeta potentials as low as 0 mV, colloidal systems with steric stabilizers can display good long-term stability<sup>(40)</sup>.

The drug content in F22 was 96.1%, which means that there was a low percentage of drug loss during the formulation process.

The entrapment efficiency was 98.6%. The high entrapment efficiency was due to the sufficient stabilizer concentration that entraps ACM particles. Also, acemetacin is a highly lipophilic drug that has a higher tendency to be entrapped in the lipophilic moiety of Soluplus®<sup>(41)</sup>.

F22 nanosuspension exhibited significantly faster release (58.9% in 30 minutes) compared to the pure drug dispersion (21.9%). Attributed to ACM nanosuspension ' larger surface area enhancing wettability and contact with the

dissolution medium, as per the Noyes-Whitney equation<sup>(42)</sup>.

When comparing the Fourier transform infrared spectroscopy spectrum of ACM nanosuspension to that of the pure ACM, no additional peaks were observed, indicating that there was no chemical interaction between ACM and Soluplus®.

Acemetacin's most characteristic X-ray diffraction peaks were significantly less visible in the pattern of the lyophilized ACM nanosuspension (Figure 4C), indicating a transformation of the crystalline ACM into an amorphous structure. The amorphous form is less stable than the crystalline one, but it has a higher solubility and dissolution rate<sup>(43)</sup>.

The DSC thermogram of F22 lyophilized ACM nanosuspension lacks the sharp endothermic peak at the ACM melting range, indicating that the nanosuspension was completely covered by Soluplus® and has a lower crystallinity than the pure ACM. Also, no additional peaks have shown up, suggesting that acemetacin and Soluplus® are compatible<sup>(44)</sup>.

## Conclusion

Acemetacin nanosuspension can be successfully developed using the solvent-anti-solvent approach. The smallest particle size was obtained by using Soluplus® as a stabilizer, and there was no chemical interaction between ACM and Soluplus®. As Soluplus® amount, water volume, and stirring rate increased, the particle size decreased. Turning ACM into nanosuspension is an effective method to increase the rate of dissolution of the drug. Looking ahead, the most promising nanosuspension formulation could potentially find applications in diverse drug delivery systems, encompassing oral as well as non-oral routes such as ophthalmic, parenteral, and transdermal dosage forms.

## Acknowledgment

The University of Baghdad's College of Pharmacy is acknowledged by the authors for providing the resources needed to complete this work.

## Conflicts of Interest

The authors state that there are no conflicts of interest.

## Funding

There was no special funding for this study.

## Ethics Statements

Since there were no humans or animals involved, no ethical approval was needed for this project.

## Author Contribution

The authors write, edit, and evaluate the manuscript in addition to contributing to the result analysis.

## References

1. Patravale, V. B., Date, A. A., & Kulkarni, R. M. Nanosuspensions: a promising drug delivery strategy. *Journal of Pharmacy and Pharmacology*. 2010; 56(7): 827–840. <https://doi.org/10.1211/0022357023691>
2. Chavda, H. v., Patel, C. N., & Anand, I. S. Biopharmaceutics classification system. In *Systematic Reviews in Pharmacy*. 2015;1(1):62–69. <https://doi.org/10.4103/0975-8453.59514>
3. Thomas, L. M., & Khasraghi, A. H. Nanotechnology-based topical drug delivery systems for management of dandruff and seborrheic dermatitis: An overview. In *Iraqi Journal of Pharmaceutical Sciences*. 2015; 29(1):12–32. <https://doi.org/10.31351/VOL29ISS1PP12-32>
4. Alhagies, A. W., & Ghareeb, M. M. Formulation and Characterization of Nimodipine Nanoparticles for the Enhancement of solubility and dissolution rate, *Iraqi Journal of Pharmaceutical Sciences*. 2021;30(2):143–152. <https://doi.org/10.31351/vol30iss2pp143-152>
5. Jadhav, S. P., Singh, S. K., & Chawra, H. S. Review on Nanosuspension as a Novel Method for Solubility and Bioavailability Enhancement of Poorly Soluble Drugs. *Advances in Pharmacology and Pharmacy*. 2023;11(2):117–130. <https://doi.org/10.13189/app.2023.110204>
6. Madkour, M., Bumajdad, A., & Al-Sagheer, F. To what extent do polymeric stabilizers affect nanoparticle characteristics? In *Advances in Colloid and Interface Science*. 2019; 270:38–53. Elsevier B.V. <https://doi.org/10.1016/j.cis.2019.05.004>
7. Brayfield, Alison, Martindale: The complete drug reference, thirty-eight edition, pharmaceutical press, London, 2014. P.16.3.
8. Chávez-Piña, A. E., McKnight, W., Dickey, M., Castañeda-Hernández, G., & Wallace, J. L. Mechanisms underlying the anti-inflammatory activity and gastric safety of acemetacin. *British Journal of Pharmacology*. 2007; 152(6):930–938. <https://doi.org/10.1038/sj.bjp.0707451>
9. Sanphui, P., Bolla, G., Nangia, A., & Chernyshev, V. Acemetacin cocrystals and salts: Structure solution from powder X-ray data and form selection of the piperazine salt. *IUCrJ*. 2014;1:136–150. <https://doi.org/10.1107/S2052252514004229>
10. Aybaba, C., Palabiyik, I. M., Caglayan, M. G., & Onur, F. Multivariate optimization of separation conditions for simultaneous determination of acemetacin and chlorzoxazone in a pharmaceutical preparation by HPLC using Response surface methodology. *Journal of AOAC International*. 2013; 96(4): 723–729. <https://doi.org/10.5740/jaoacint.11-092>
11. Shehata, T. M., Abdallah, M. H., & Ibrahim, M. M. Proniosomal Oral Tablets for Controlled Delivery and Enhanced Pharmacokinetic Properties of Acemetacin. *AAPS PharmSciTech*. 2014; 16(2):375–383. <https://doi.org/10.1208/s12249-014-0233-5>
12. Mona A. Shewaiter, Adli A. Selim, Yasser M. Moustafa, Shadeed Gad, Hassan M. Rashed, Radioiodinated acemetacin loaded niosomes as a dual anticancer therapy, *International Journal of Pharmaceutics*. 2022; 628. <https://doi.org/10.1016/j.ijpharm.2022.122345>
13. Adil Muhesen, R., & Ayash Rajab, N. Formulation and Characterization of Olmesartan medoxomil as a Nanoparticle. *Research Journal of Pharmacy and Technology*. 2023; 3314–3320. <https://doi.org/10.5271/1/0974-360X.2023.00547>
14. Kassab, H. J., Alkufi, H. K., & Hussein, L. S. Use of factorial design in formulation and evaluation of intrarectal in situ gel of sumatriptan. *Journal of Advanced Pharmaceutical Technology and Research*. 2023; 14 (2):119–124. <https://doi.org/10.4103/japtr.japtr.603.22>
15. Alfaris, R., & K Al-Kinani, K. Preparation and Characterization of Prednisolone Acetate Microemulsion for Ophthalmic Use. *Journal of the Faculty of Medicine Baghdad*. 2023;65(3):205–211. <https://doi.org/10.32007/jfacmedbagdad.2045>
16. Naji, G. H., & al Gawhari, F. J. Study the Effect of Formulation Variables on Preparation of Nisoldipine Loaded Nano Bilosomes. *Iraqi Journal of Pharmaceutical Sciences*. 2023; 32:271–282. <https://doi.org/10.31351/vol32issSuppl.pp271-282>
17. Abdullah, T., & Al-Kinani, K. Propranolol nanoemulgel: Preparation, in-vitro and ex-vivo characterization for a potential local hemangioma therapy. *Pharmacia*. 2024;71:1–12. <https://doi.org/10.3897/pharmacia.71.e115330>
18. Qi, X., Jiang, Y., Li, X., Zhang, Z., & Wu, Z. Zero-order release three-layered tablet with an acemetacin solid dispersion core and a hydroxypropyl methylcellulose capped matrix. *Journal of Applied Polymer Science*. 2015; 132 (24). <https://doi.org/10.1002/app.42059>
19. Mokarram, R. A., & zadeh, K. A. Preparation and in-vitro evaluation of indomethacin nanoparticles. *DARU Journal of Pharmaceutical Sciences*. 2010; 18(3):185–192.
20. Al-Obaidy, R. A. R., & Rajab, N. A. Preparation and In-vitro Evaluation of Darifenacin HBr as Nanoparticles Prepared as Nanosuspension. *International Journal of Drug Delivery Technology*. 2022; 12(2): 775–781. <https://doi.org/10.25258/ijddt.12.2.55>
21. Rashid, A. M., & Abd-Alhammid, S. N. Formulation and characterization of itraconazole as nanosuspension dosage form for enhancement

- of solubility. *Iraqi Journal of Pharmaceutical Sciences*. 2019; 28(2):124–133. <https://doi.org/10.31351/vol28iss2pp124-133>
22. Salman, A. H., Al-Gawhari, F. J., & Al-kinani, K. K. (2021). The effect of formulation and process variables on prepared etoricoxib Nanosponges. *Journal of Advanced Pharmacy Education and Research*. 2021;11 (2):82–87. <https://doi.org/10.51847/QOQRKUV2kQ>
  23. Kaur, A., Khodabhai Parmar, P., & Kumar Bansal, A. Evaluation of different techniques for size determination of drug nanocrystals: A case study of celecoxib nanocrystalline solid dispersion. *Pharmaceutics*. 2019; 11(10). <https://doi.org/10.3390/pharmaceutics11100516>
  24. Guo, J. J., Yue, P. F., Lv, J. L., Han, J., Fu, S. S., Jin, S. X., Jin, S. Y., & Yuan, H. L. Development and in vivo/in vitro evaluation of novel herpentrione nanosuspension. *International Journal of Pharmaceutics*. 2013; 441(1–2):227–233. <https://doi.org/10.1016/j.ijpharm.2012.11.039>
  25. Abdullah, T. M., & Al-Kinani, K. K. Topical Propranolol Hydrochloride Nanoemulsion: A Promising Approach Drug Delivery for Infantile Hemangiomas. *Iraqi Journal of Pharmaceutical Sciences*. 2023; 32: 300–315. <https://doi.org/10.31351/vol32issSuppl.pp300-315>
  26. Pandya, V., & Patel, D. Formulation, Optimization and characterization of Simvastatin Nanosuspension prepared by nanoprecipitation technique. *Der Pharmacia Lettre*, 2011; 3(2) :129 - 140. DOI: [10.14227/DT180311P40](https://doi.org/10.14227/DT180311P40)
  27. Gao, L., Zhang, D., & Chen, M. Drug nanocrystals for the formulation of poorly soluble drugs and its application as a potential drug delivery system. In *Journal of Nanoparticle Research*. 2008;10(5):845–862. <https://doi.org/10.1007/s11051-008-9357-4>
  28. Danaei, M., Dehghankhold, M., Ataei, S., Hasanzadeh Davarani, F., Javanmard, R., Dokhani, A., Khorasani, S., & Mozafari, M. R. Impact of particle size and polydispersity index on the clinical applications of lipidic nanocarrier systems. In *Pharmaceutics*. 2018;10(2). MDPI AG. <https://doi.org/10.3390/pharmaceutics10020057>
  29. Akram, W., Garud, N. Design expert as a statistical tool for optimization of 5-ASA-loaded biopolymer-based nanoparticles using Box Behnken factorial design. *Futur J Pharm Sci*. 2021; 7:146. <https://doi.org/10.1186/s43094-021-00299-z>
  30. Albash, R., El-Nabarawi, M. A., Refai, H., & Abdelbary, A. A. Tailoring of PEGylated bilosomes for promoting the transdermal delivery of olmesartan medoxomil: Invitro characterization, ex-vivo permeation and in-vivo assessment. *International Journal of Nanomedicine*. 2019; 14:6555–6574. <https://doi.org/10.2147/IJN.S213613>
  31. Teng, M., Li, J., Li, Z., Zhang, G., Zhao, P., & Fu, Q. Recrystallization Mediates the Gelation of Amorphous Drugs: The Case of Acemetacin. *Pharmaceutics*. 2023.; 15(1). <https://doi.org/10.3390/pharmaceutics15010219>
  32. Afzal, A., Thayyil, M. S., Sivaramakrishnan, P. A., Sulaiman, M. K., Hussan, K. P. S., Panicker, C. Y., & Ngai, K. L. Dielectric spectroscopic studies in supercooled liquid and glassy states of Acemetacin, Brucine and Colchicine. *Journal of Non-Crystalline Solids*. 2019;508:33–45. <https://doi.org/10.1016/j.jnoncrsol.2019.01.008>
  33. AlSheyyab RY, Obaidat RM, Altall YR, Abuhuwaj RT, Ghanma RR, Ailabouni AS, et al. Solubility enhancement of Nimodipine through preparation of Soluplus® dispersions. *J Appl Pharm Sci*. 2019; 9(9):30–37. DOI:[10.7324/JAPS.2019.90905](https://doi.org/10.7324/JAPS.2019.90905)
  34. Moffat, Osselton, Widdop: *Clarcks analysis of drugs and poisons*, Fourth edition, pharmaceutical press, London, 2011.; P.2347
  35. Yang, H., Teng, F., Wang, P., Tian, B., Lin, X., Hu, X., Zhang, L., Zhang, K., Zhang, Y., & Tang, X. Investigation of a nanosuspension stabilized by Soluplus® to improve bioavailability. *International Journal of Pharmaceutics*. 2014; 477(1–2):88–95. <https://doi.org/10.1016/j.ijpharm.2014.10.025>
  36. Hao, J., Gao, Y., Zhao, J., Zhang, J., Li, Q., Zhao, Z., & Liu, J. Preparation and Optimization of Resveratrol Nanosuspensions by Antisolvent Precipitation Using Box-Behnken Design. *AAPS PharmSciTech*. 2014; 16(1):118–128. <https://doi.org/10.1208/s12249-014-0211-y>
  37. Du, J., Zhou, Y., Wang, L., & Wang, Y. Effect of PEGylated chitosan as multifunctional stabilizer for deacetyl mycoepoxydiene nanosuspension design and stability evaluation. *Carbohydrate Polymers*. 2016; 153:471–481. <https://doi.org/10.1016/j.carbpol.2016.08.002>
  38. Bajaj, A., Rao, M. R. P., Pardeshi, A., & Sali, D. Nanocrystallization by evaporative antisolvent technique for solubility and bioavailability enhancement of telmisartan. *AAPS PharmSciTech*. 2012; 13(4):1331–1340. <https://doi.org/10.1208/s12249-012-9860-x>
  39. Mohamed S. Attia, Ahmed Elshahat, Ahmed Hamdy, Ayman M. Fathi, Mahmoud Emad-Eldin, Fakhreldin S. Ghazy, Hitesh Chopra, Tarek M. Ibrahim, Soluplus® as a solubilizing excipient for poorly water-soluble drugs: Recent advances in formulation strategies and pharmaceutical product features. *Journal of Drug Delivery Science and Technology*. 2023; 84.
  40. Uddhav S Bagul, Vrushali V Pisal, Nachiket V Solanki, Antara Karnavat. Current Status of

- Solid Lipid Nanoparticles: A Review. Mod Appl Bioequiv Availab. 2018; 3(4): 1-10.
41. Sable, P., Lahoti, S., Ghadalinge, S., & Sangshetti, J. Formulation and Development of Nanosuspension For Solubility Enhancement Of Gefitinib. Journal of Pharmaceutical Negative Results. 2022;13. <https://doi.org/10.47750/pnr.2022.13.S10.454>
42. A. S. Noyes W. R. Whitney. The rate of solution of solid substances in their own solutions J. Am. Chem. 1897. Soc. 19:930–934
43. Raut M, Mahajan DT, Sakharkar DM, Bodke PS. Water and Temperature Induced Polymorphic Transformations of Mannitol. International Journal of Current Research .2011; 3(12) :169-172.
44. Zhang, K., Yu, H., Luo, Q., Yang, S., Lin, X., Zhang, Y., Tian, B., & Tang, X. Increased dissolution and oral absorption of itraconazole/Soluplus extrudate compared with itraconazole nanosuspension. European Journal of Pharmaceutics and Biopharmaceutics. 2013;85(3):1285–1292. <https://doi.org/10.1016/j.ejpb.2013.03.002>

## صياغة وتقييم خارج الجسم للمعلق النانوي للاسيميتاسين حسين الغراني<sup>1</sup> و خالد الكناني<sup>2,\*</sup>

<sup>1</sup> وزارة الصحة ، دائرة صحة كربلاء، كربلاء، العراق.

<sup>2</sup> فرع الصيدلانيات، كلية الصيدلة، جامعة بغداد، بغداد، العراق.

### الخلاصة

الاسيميتاسين هو مضاد التهاب غير ستيرويدي. وهو استر جلايكوليك لعقار الاندوميثاسين حيث يتحول الى الاندوميثاسين داخل الجسم الحي. يعمل الاسيميتاسين كمضاد التهاب مسكن للالم و خافض للحرارة بسبب تثبيطه لعمل البروستاجلاندينات. يعتبر الاسيميتاسين عقار من الصنف الثاني حيث يمتاز بذوبانيته القليلة ونفاذيته العالية. يهدف البحث الى تحضير الاسيميتاسين على شكل معلق نانوي لغرض تعزيز معدل الذوبان. حيث تم تكوين المعلق النانوي باستخدام تقنية الترسيب للمذيب ومضاد المذيب. تم استخدام نوعين من المثبتات لتحضير المعلق النانوي للاسيميتاسين وهما السوليوبلس و ديوكسي كولات الصوديوم. تم اذابة الاسيميتاسين في الايثانول و اضافته عن طريق التقطير الى مضاد المذيب الحاوي على المادة المثبتة والموضوعة على الخلاط المغناطيسي. تم استخدام التصميم التجريبي القائم على الكومبيوتر حيث تم اختيار تصميم بوكس بينكن لغرض معرفة تأثير متغيرات الصياغة المختلفة على حجم جزيئات المعلق النانوي ومقياس التشتت المتعدد. اظهرت النتائج ان السوليوبلس هو الافضل بتقليل حجم الجزيئات وان قيمة الرغية للصيغة الثانية والعشرون هي 0.701 وحجم جزيئاتها (59,69) نانوميتر ومقياس تشتت متعدد 1847. تضاعفت قيمة الذوبانية بمقدار عشرة مرات وقد حققت الصيغة الثانية والعشرون معدل ذوبان 58,9% خلال 30 دقيقة بينما كان معدل ذوبان الاسيميتاسين الخام بنسبة 21,9% خلال نفس المدة. وبذلك نستنتج ان تحضير الاسيميتاسين على شكل معلق نانوي قد حسن من معدل ذوبان الاسيميتاسين ليكون جاهزا للدمج في الاشكال الدوائية التي تتطلب مثل هذه الخصائص.

الكلمات المفتاحية : المعلق النانوي للاسيميتاسين ، تصميم بوكس بينكن ، ديوكسي كولات الصوديوم ، سوليوبلس ، المذيب و مضاد المذيب.